

Cite this: *New J. Chem.*, 2012, **36**, 1762–1768

www.rsc.org/njc

PAPER

Enhancing selectivity in photocatalytic formation of *p*-anisaldehyde in aqueous suspension under solar light irradiation *via* TiO₂ N-doping†

Sedat Yurdakal,^{*a} Vincenzo Augugliaro,^b Vittorio Loddo,^b Giovanni Palmisano^b and Leonardo Palmisano^{*b}

Received (in Montpellier, France) 15th May 2012, Accepted 9th June 2012

DOI: 10.1039/c2nj40394c

The photocatalytic partial oxidation of 4-methoxybenzyl alcohol to the corresponding aldehyde (*p*-anisaldehyde) was performed under simulated solar irradiation by using home prepared N-doped TiO₂ catalysts. The photocatalysts were prepared by a sol–gel method, using TiCl₄ as TiO₂ precursor and NH₄Cl, urea or NH₄OH as N-doping sources. A commercial TiO₂ (Degussa P25) was also used for comparison aims. The prepared catalysts were characterized by BET specific surface area, XRD, ESEM and UV-vis spectroscopy. The reactivity results show that (i) the doped catalysts are predominantly amorphous, and they show selectivity values far higher than those of the corresponding undoped ones and of well crystallized catalysts – even if the last ones show a higher activity – and (ii) exploitation of solar light significantly increases the reaction selectivity. In addition, different light sources were also used in order to investigate the effect of radiation wavelength ranges on the reactivity and selectivity to aldehyde.

1 Introduction

Among the various semiconductor materials tested as oxidation photocatalysts, TiO₂ has shown to be the most reliable one due to its low cost, high photostability and activity.^{1–3} Owing to the fact that TiO₂ excitation occurs only under near-UV radiation and that only a small aliquot (2–3%) of solar radiation reaching the Earth is in the UV region, researchers have tried to modify the titania catalysts in order to make them able to absorb radiation of the visible region.⁴ Once this type of photocatalysts is at disposal, the cheap and renewable solar energy could also be used for photocatalytic syntheses of organic compounds.

In order to reduce TiO₂ band gap energy, it is very common to dope it with some non-metal atoms, such as N, S, C, P and F;⁵ among these the most active doping is that carried out with nitrogen, as its size is similar to that of oxygen.

N-doped TiO₂ catalysts (N–TiO₂) can be prepared by three different methods: spraying and implantation, sinterization at high temperature and sol–gel method; this last one is the most

successful method⁵ because it allows an easy control of nitrogen amount and of catalyst particle sizes.

Even though most of N–TiO₂ catalysts have been used for degradation of harmful compounds under visible irradiation,^{6–11} a few investigations have been devoted to carry out organic syntheses with these catalysts.^{12,13} All these works but one¹⁴ have been carried out by using organic solvents. The choice of organic solvents instead of water is due to the low solubility of most of organic molecules in water and to the generally low selectivity of the photocatalytic organic syntheses in water because they involve the formation of hydroxyl radicals.^{2,3}

Selective oxidation of hydroxyl groups to carbonyl ones can be considered a key step in many organic syntheses. In the industrial practice this process is usually catalytic and it is carried out in the presence of organic solvents at high temperature and pressure as well as of stoichiometric oxygen donors (such as chromate and permanganate) that are not only expensive and toxic, but also produce large amounts of dangerous waste. Hence, one of the main goals of current research is that of eliminating the environmentally harmful conditions of industrial processes.^{15,16}

Only recently, photocatalytic partial oxidation of aromatic alcohols to the corresponding aldehydes has been carried out under near-UV radiation in aqueous suspensions of home-prepared (HP) anatase,^{17–19} brookite^{20,21} and rutile TiO₂^{22–24} in laboratory batch reactors and also in continuous reactors.^{25,26} In those conditions HP photocatalysts showed selectivity values for aldehyde production far higher than those of commercial TiO₂ ones.

In order to find likely explanations for the different photocatalytic performances shown by HP and commercial catalysts,

^a Kimya Bölümü, Fen-Edebiyat Fakültesi, Afyon Kocatepe Üniversitesi, Ahmet Necdet Sezer Kampüsü, 03100, Afyonkarahisar, Turkey. E-mail: sedatyurdakal@gmail.com; Fax: +90 272 228 12 35; Tel: +90 272 228 1339/230

^b “Schiavello-Grillone” Photocatalysis Group, Dipartimento di Ingegneria Elettrica, Elettronica e delle Telecomunicazioni, di tecnologie Chimiche, Automatica e modelli Matematici, University of Palermo, Viale delle Scienze, 90128 Palermo, Italy. E-mail: leonardo.palmisano@unipa.it

† Dr S. Yurdakal thanks the TÜBİTAK (Project no: 111T489) for financial support.

their textural, bulk and surface properties have been investigated.^{18,19} It was found that the textural and intrinsic electronic features of catalysts were almost the same; on the contrary ATR-FTIR studies indicated that the higher selectivity found for HP catalysts with respect to commercial ones is related to their low crystallinity and to their high surface hydroxyl group density that induces an enhanced hydrophilicity of the TiO₂ surface. Both of these properties promote desorption of the photo-produced aldehyde, thus hindering its further oxidation.

To best of our knowledge the unique work about selective oxidation with N-doped TiO₂ under visible light and in water is that of Sivarajani and Gopinath.¹⁴ In this study selective oxidation of 4-methoxybenzyl alcohol (MBA) to *p*-anisaldehyde (PAA) was carried out successfully in aqueous solution by using N-doped wormhole mesoporous TiO₂ under direct sunlight. After 7 hours irradiation at wavelengths higher than 420 nm, a 30.2% yield of aldehyde was obtained. The high activity of the photocatalyst under direct sunlight, in spite of a high band gap (3.24 eV), is attributed to the better utilization of holes due to the low charge diffusion barrier associated with wormhole mesoporosity along with the high crystallinity of nanoparticulate TiO_{2-x}N_x.

Recently, Bellardita *et al.*⁹ reported various sol-gel methods for the preparation of N-doped TiO₂ catalysts to be used for the degradation of 4-nitrophenol in water under visible irradiation. Different percentages of nitrogen and different kinds of precursors were tested for these preparations. The efficacy of the preparation method for the N-doping was successfully checked by Raman spectroscopy and X-ray photoelectron spectroscopy. The doped powders exhibited two absorption edges: the main one due to TiO₂ and the second one due to the presence of a localized midgap band that induces the visible light activity. The highest photoactivity was shown by an ex TiCl₄ TiO₂ catalyst with 2 at% of nitrogen derived from NH₄Cl.

The present work has been devoted to investigate the influence of TiO₂ N-doping on selectivity of photocatalytic oxidation of MBA to PAA in water under simulated solar irradiation. The catalysts have been synthesized by the sol-gel method, characterized by BET specific surface area, XRD, ESEM and UV-vis spectroscopy and tested in a batch photoreactor. By following Bellardita *et al.*'s results⁹ on the optimal concentration of N-doping, different catalysts have been prepared with a fixed nitrogen content of 2 at% but at different boiling times of native suspension, calcination temperatures and nitrogen sources. Moreover the influence of different radiation sources (near-UV, visible light or simulated solar radiation) on the photoprocess performance has been investigated.

2 Experimental

2.1 Catalyst preparation and characterization

The precursor solution was obtained by adding 20 mL of TiCl₄ (purity >97%, Fluka), drop by drop under magnetic agitation, to 200 mL of deionised water contained in a 500 mL beaker placed inside an ice bath. After that the beaker was sealed and mixing was prolonged for 12 h at room temperature, eventually obtaining a clear solution. Fixed amounts of nitrogen sources (NH₄Cl, NH₃ or urea) were dissolved in 125 mL of this solution; the nitrogen content was calculated as the ratio between the weight of nitrogen and that of TiO₂. The resulting

solution was magnetically stirred and refluxed for different times (0.1, 2, 5, and 8 h) at 100 °C in a flask fitted with a Graham condenser. The reflux zero time was considered that for which the solution left its transparency. The obtained suspension was then dried at 50 °C by means of a rotary evaporator machine (Buchi model M) working at 50 rpm, in order to obtain the final powdered catalysts. In a few cases the powder was calcined at 400 °C to obtain crystalline catalysts. The obtained catalysts are hereafter named N-HPX-Y-400, in which N indicates nitrogen, X the duration of suspension heating at 100 °C, Y the name of nitrogen source and "400" is used only if the catalyst was calcined at 400 °C.

A blank catalyst was also prepared by following the previously described procedure but without adding any nitrogen source; it is named HP2, being 2 the hours of suspension heating at 100 °C.

A rutile TiO₂ sample was also home-prepared. The precursor solution was obtained by adding 20 mL of TiCl₄ to 1000 mL of water contained in a volumetric flask (2 L). At the end of the addition, the resulting solution was stirred for 2 min by a magnetic stirrer and then the flask was sealed and maintained at room temperature (*ca.* 25 °C) for a total aging time of 6 days. After *ca.* 12 h from the starting of aging, the sol became almost transparent and then, after waiting for a few (2 or 3) days, the precipitation process started. The solid powder, precipitated at the end of the treatment, was separated by centrifugation (20 min at 5000 rpm) and dialysed several times with deionised water until a neutral pH was reached. Then the sample was again centrifuged and dried at room temperature. The final home-prepared catalyst is hereafter denoted HPRT.

XRD patterns of the powders were recorded by a Philips diffractometer using the Cu K α radiation and a 2 θ scan rate of 1.28° min⁻¹. SEM images were obtained using an ESEM microscope (Philips, XL30) operating at 25 kV. A thin layer of gold was evaporated on the catalysts samples, previously sprayed on the stub and dried at room temperature. BET specific surface areas were measured by the single-point BET method using a Micromeritics Flow Sorb 2300 apparatus. Before the measurement, the samples were dried for 1 h at 100 °C, for 2 h at 150 °C and degassed for 0.5 h at 150 °C.

Visible-Ultraviolet spectra were obtained by diffuse reflectance spectroscopy using a Shimadzu UV-2401 PC instrument. BaSO₄ was used as a reference and the spectra were recorded in the range of 300–600 nm.

2.2 Photoreactivity setup and procedure

A cylindrical Pyrex batch photoreactor with an immersed lamp, containing 0.150 L of aqueous suspension, was used to perform the reactivity experiments both under visible and near-UV light. The photoreactor was provided with open ports in its upper section for contacting the suspension with the atmosphere and for sampling. A magnetic stirrer guaranteed a satisfactory suspension of the photocatalyst and the homogeneity of the reacting mixture. A 125 W medium pressure Hg lamp (Helioquartz, Italy) or a 100 W halogen display lamp (Osram, Germany) was axially positioned within the photoreactor; it was cooled by water circulating through a Pyrex thimble surrounding the lamp. The temperature of the suspension was about 27 °C. When the medium pressure Hg lamp was used the radiation

Table 1 Features of the light sources

Light source	Light irradiance	Light irradiance	Reactor geometry
	315–400 nm (mW cm ⁻²)	450–950 nm (mW cm ⁻²)	
Solar box	0.79	86	Cylindrical
Visible light (100 W)	0.20	200	Annular
UV light (125 W)	12.20	100	Annular

energy impinging on the suspension had an average value of 12.20 mW cm⁻² in the 315–400 nm range and of 100 mW cm⁻² in the 450–950 nm range, whereas the halogen display lamp gave corresponding values of 0.2 and 200 mW cm⁻², respectively. The radiation energy values were measured by using a radiometer (Delta Ohm, DO 9721).

A 1500 W solar light simulator (Solarbox) was employed for the runs carried out under simulated solar radiation. The distance from the lamp to the suspension was 27.5 cm. The radiation energy impinging on the suspension had an average value of 0.79 mW cm⁻² (in 315–400 nm range) and 86 mW cm⁻² (in 450–950 nm range). The irradiance values of all of the used light sources are reported in Table 1. A 250 mL cylindrical beaker (diameter: 6.7 cm) containing 150 mL of aqueous suspension was used as photo-reactor. A magnetic stirrer guaranteed a satisfactory suspension of the photocatalyst and the homogeneity of the reacting mixture.

The MBA initial concentration was 0.6 mM and the catalyst amount was 0.6 g L⁻¹. This amount guaranteed that all the catalyst particles were irradiated. Light transmittance was indeed measured at the reactor wall and *ca.* 90% of the emitted irradiance was cut, thus demonstrating that not all the emitted photons were screened by the suspension. Before switching on the lamp, the suspension was stirred for 30 min at room temperature in order to reach the thermodynamic equilibrium. The contact of the suspension with the atmosphere guaranteed that the aqueous solution was saturated by oxygen.

During the run, samples of reacting suspension were withdrawn at fixed time intervals; they were immediately filtered through a 0.20 µm hydrophilic membrane (HA, Millipore) before being analysed.

The quantitative determination and identification of the species present in the reacting suspension was performed by means of a Beckman Coulter HPLC (System Gold 126 Solvent Module and 168 Diode Array Detector), equipped with a Phenomenex Synergi 4 µm Hydro-RP 80A column at 25 °C, using Sigma Aldrich standards. Retention times and UV spectra of the compounds were compared with those of standards. The eluent consisted of 55% methanol and 45% 1 mM trifluoroacetic acid aqueous solution. The flow rate was 0.4 cm³ min⁻¹. TOC analyses were carried out by using a 5000 A Shimadzu TOC analyser. All the used chemicals were purchased from Sigma Aldrich with a purity >98.0%.

3 Results and discussion

3.1 Characterization of the photocatalysts

In the XRD diffractograms of titania the peaks at $2\theta = 27.5^\circ$, 36.5° , 41° , 54.1° and 56.5° are characteristic of rutile and those at $2\theta = 25.58$, 38.08 , 48.08 , 54.58 of anatase. Fig. 1 shows XRD patterns of the home-prepared and commercial TiO₂ photocatalysts. The HP catalysts are in the anatase, rutile or anatase–rutile phases; all of the samples prepared at room temperature (HPRT) or at low temperature (100 °C) show broad crystalline peaks, indicating that the samples have a low degree of crystallinity and are mainly constituted by amorphous phase. Anatase crystals are present in the HP2, N-HP0.1-NH₄Cl, N-HP2-Urea and N-HP2-NH₄OH samples while rutile crystals in the HPRT and N-HP8-NH₄Cl samples; all the other specimens are a mixture of anatase and rutile. The increase of the boiling time of the N-HP-NH₄Cl catalyst

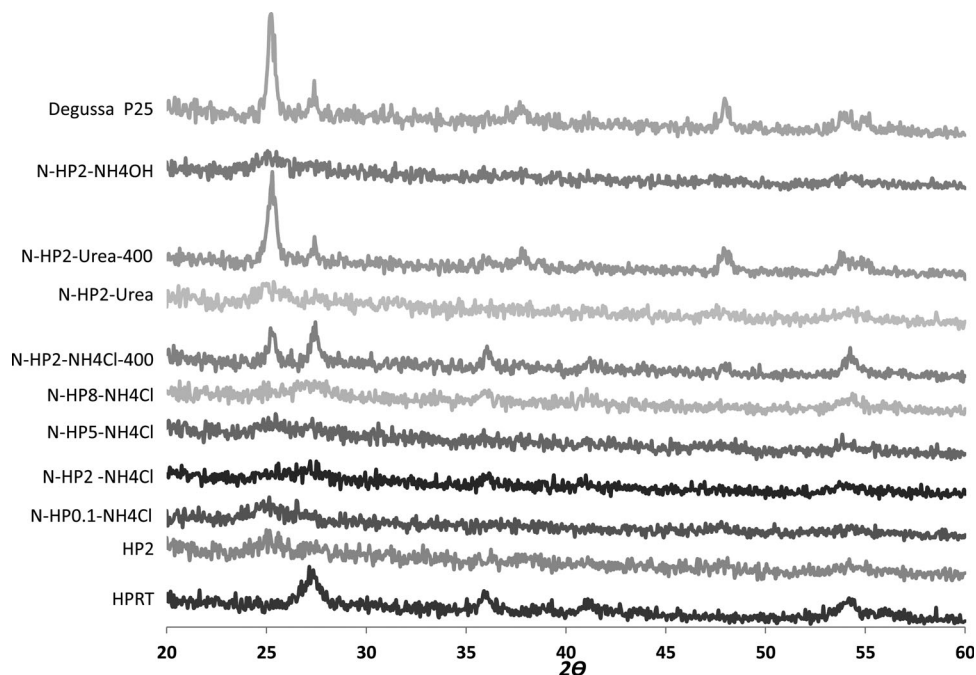
**Fig. 1** XRD patterns of home-prepared and commercial TiO₂ photocatalysts.

Table 2 Crystallite phase, BET specific surface area (SSA), particle size crystallite sizes and band gap energies of the photocatalysts

Catalyst	Crystalline phase	SSA/ m ² g ⁻¹	Anatase crystals size/nm	Rutile crystals size/nm	Band gap energy/eV
HP2	A	189	3.6	—	2.98
HPRT	R	105	—	6.8	3.01
N-HP0.1-NH ₄ Cl	A	179	3.4	—	2.97
N-HP2-NH ₄ Cl	A + R	132	3.9	6.5	2.95
N-HP5-NH ₄ Cl	A + R	128	4.5	10.2	2.93
N-HP8-NH ₄ Cl	R	118	—	4.8	2.94
N-HP2-NH ₄ Cl-400	A + R	27	22.7	16.3	2.88
N-HP2-Urea	A	189	4.1	—	2.94
N-HP2-Urea-400	A + R	48	17.7	18.2	2.89
N-HP2-NH ₄ OH	A	189	4.3	—	2.93
Degussa P25	A + R	50	26.5	18.2	3.00

determines the formation of rutile crystals and the contemporary transformation of anatase crystals to rutile which is the most stable crystalline phase. The N-HP2-Urea-400 and N-HP2-NH₄Cl-400 samples are very crystalline due to the calcination treatment at a temperature of 400 °C. These samples are a mixture of anatase and rutile; HP2-NH₄Cl-400 has similar amounts of these two phases while N-HP2-Urea-400 shows almost the same XRD pattern of Degussa P25 (*ca.* 80% anatase, 20% rutile). It must be stressed that the thermal treatment at moderate temperature is able to transform the predominantly amorphous samples in predominantly crystalline samples.

For the samples prepared at low temperature the values of the primary crystallite sizes (4.8–10.2 nm, calculated using the Scherrer equation) were lower than those (16.3–18.2 nm) of the samples prepared at high temperature and of the commercial ones (see Table 2). The size of the aggregates of the crystalline catalysts was quite high and ranged between *ca.* 20 and 80 nm, as estimated from SEM observations; the lowest values were found when samples were thermally treated. Accordingly Fig. 2 shows that sample N-HP2-Urea is subjected to particles sintering when calcined at 400 °C. BET specific surface areas of predominantly amorphous samples (average value: 150 m² g⁻¹) are much higher than those of crystalline samples (average value: 45 m² g⁻¹). This strong decrease of surface area is clearly due to particles growth and sintering effects occurring at the temperature of treatment.

UV-visible spectra of the photocatalysts are reported in Fig. 3. All the catalysts show a poor absorbance in the visible region except the N-HP2-NH₄Cl-400 and N-HP2-Urea-400 samples; these catalysts absorb radiation with wavelength as high as 540 nm while the absorbance of the others stops at 410–420 nm. Among the N-doped samples, only these two samples are crystalline and could be used under visible light irradiation. For the excitation of the other catalysts both UV and visible radiation is needed as it is the case of solar light. Band gap energies of the samples were determined by using their UV-absorbance spectra; the corresponding values are reported in Table 2. Undoped samples present wide band gap energies (*ca.* 3 eV), while both predominantly amorphous and crystalline N-doped TiO₂ samples have narrow band gap energies, *ca.* 2.94 and 2.88, respectively. These results also stress the point that only N-doped crystalline TiO₂ samples could be used as photocatalysts under visible irradiation. The band gap energies of predominantly amorphous and crystalline samples clearly indicate that the doping of the TiO₂ structure by nitrogen atoms occurred during the boiling treatment and it also increased during calcination.

3.2 Photoreactivity

No oxidation of alcohols was observed in the absence of irradiation, catalyst or oxygen for runs carried out under the same experimental conditions used for the photocatalytic ones. Irradiation, catalyst and oxygen were all needed for the occurrence of the process.

Adsorption of the alcohol under dark conditions was always quite low, *i.e.* less than 5%. For all the used catalysts the main products of MBA photocatalytic oxidation were the corresponding aldehyde and CO₂; this last compound was detected from the start of irradiation, thus confirming that the mineralization of adsorbed alcohol molecules occurs by means of subsequent oxidative steps, producing species which do not desorb from the photocatalyst surface into the solution. Small amounts or traces of hydroxylated aromatics, corresponding benzoic acid and opening products were also found.²³ The amounts of these last products depended on the used photocatalyst; in the presence of mainly amorphous catalysts only traces of them were found

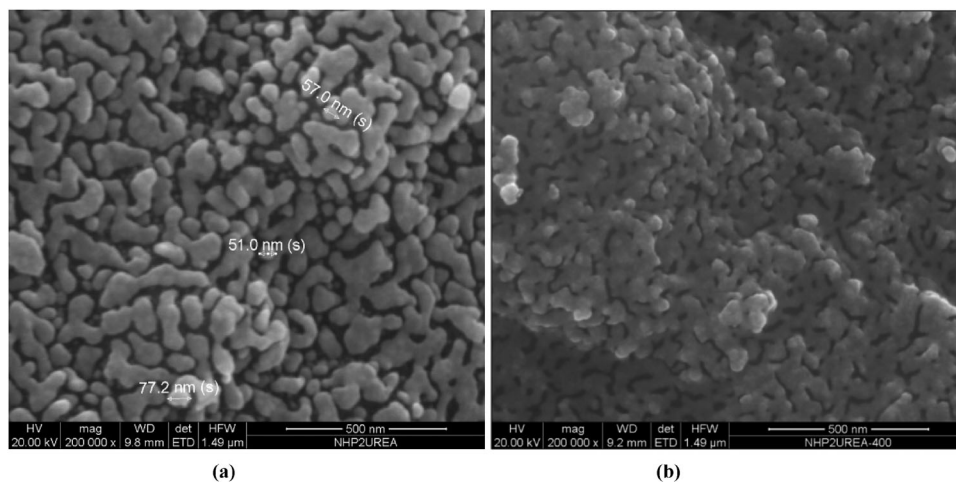


Fig. 2 SEM image (magnification: X200000) of N-HP2-Urea (a) and N-HP2-Urea-400 (b) photocatalysts.

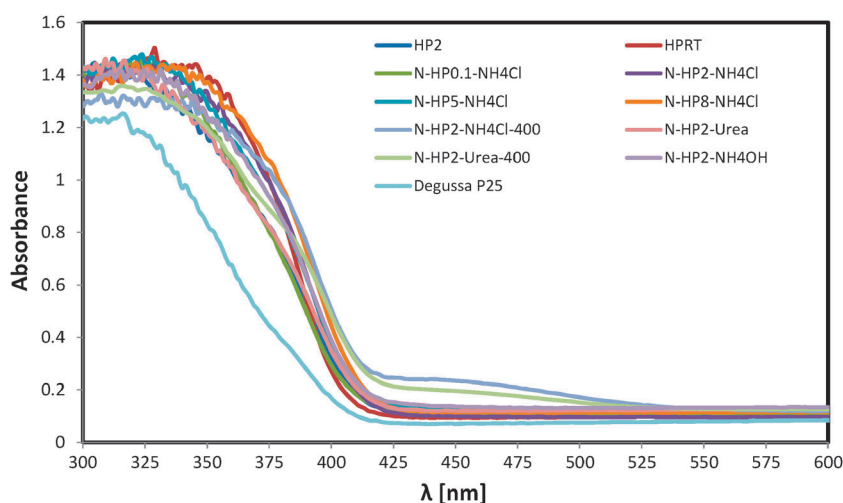


Fig. 3 UV-vis spectra of the TiO₂ photocatalysts.

whereas the crystalline ones (N-HP2-NH₄Cl-400, N-HP2-Urea-400 and Degussa P25) gave rise to higher amounts. These products obviously arise from the subsequent oxidation of produced aldehyde, being this pathway more relevant for the less selective and therefore more oxidizing samples. As the determination of the MBA oxidation mechanism was out of the aim of this paper, a thorough investigation of all the intermediates produced in the course of the photoprocess was not carried out.

The finding that the mineralization of adsorbed MBA molecules proceeds through steps in which the oxidation products are not released to the liquid phase suggests that this process should be favoured by using a catalyst with a hydrophobic surface.^{18,19,21} It has been reported^{18,21} that low crystalline catalysts have a hydrophilic surface while very crystalline catalysts have a hydrophobic surface. The hydrophilic/hydrophobic character is linked to the density of hydroxyl groups on the titania surface; this density decreases by increasing the treatment temperature of the catalyst.²¹

For the runs performed under visible light irradiation, Table 3 reports the photoreactivity results, *i.e.* the selectivity to aldehyde (calculated as the ratio between the produced moles of aldehyde and the reacted moles of alcohol) for 10% MBA conversion, the irradiation time needed for 10% MBA conversion, the MBA conversion after 3.5 h irradiation and the initial oxidation rate of MBA. This last parameter, r_0 , has been determined by the following equation:

$$r_0 = \left(-\frac{1}{S} \frac{dN_{\text{MBA}}}{dt} \right)_0 = \frac{V}{S} \left(-\frac{dC_{\text{MBA}}}{dt} \right)_0 \quad (1)$$

in which N_{MBA} indicates the MBA moles, t the irradiation time, S the specific surface area, V the suspension volume and C_{MBA} the MBA concentration. Due to the low light absorption of the samples under visible irradiation, the reaction rates were quite slow and therefore the reactivity results are analysed for 10% conversion of MBA. Notably the highest selectivity to PAA (83%) was exhibited by the N-HP2-NH₄Cl sample. N-HP2-NH₄Cl showed a higher selectivity and a little higher MBA disappearance rate with respect to the HP2 sample, prepared in the same way as N-HP2-NH₄Cl but without adding nitrogen sources. By considering that the photoreactivity runs

Table 3 Reactivity results obtained under visible light irradiation

Catalysts	$Y^a/\text{mol}\%$	t^b/h	$X^c/\text{mol}\%$	$r_0^d/\text{mmol h m}^{-2}$
Degussa P25	30	0.65	25	0.00294
HP2	69	1.5	21	0.00041
N-HP2-NH ₄ Cl	83	1.8	20	0.00043
N-HP2-NH ₄ Cl-400	27	3.8	9.3	0.00118
N-HP2-NH ₄ OH	67	1.7	20	0.00033
N-HP2-Urea	67	2.2	12	0.00027
N-HP2-Urea-400	28	2.1	16	0.00094

^a Selectivity for 10% MBA conversion. ^b Irradiation time for 10% MBA conversion. ^c MBA conversion after 3.5 h irradiation. ^d Initial oxidation rate of MBA.

have been carried out at equal rate of absorbed photons, these findings suggest that nitrogen in the bulk of titania improves the reaction rate and that the presence of nitrogen on the catalyst surface reduces the mineralization sites, therefore increasing the selectivity. The N-HP2-NH₄Cl-400 sample, prepared by calcining N-HP2-NH₄Cl, showed a far higher photoactivity but a lower selectivity than the N-HP2-NH₄Cl sample. By considering that only the N-HP2-NH₄Cl-400 sample shows a good absorbance under visible irradiation, the reactivity results indicate that the calcination treatment improves the reaction rate by improving the sample crystallinity but it partially deactivates the catalyst sites able for partial oxidation reaction. For the other N-HP2 catalysts the N-doping does not affect the selectivity but the reaction rates decrease, suggesting that nitrogen in the bulk of titania acts as a recombination center for photogenerated e^-h^+ pairs, thus decreasing the reaction rate.²⁷ The thermal treatment of the N-HP2-Urea sample determines the same pattern as that shown by the N-HP2-NH₄Cl one. Indeed the highest MBA disappearance rate under visible irradiation is shown by the bare catalysts, *i.e.* Degussa P25 and HP2.

As far as the different nitrogen sources (NH₄Cl, NH₄OH and urea) are concerned, the reactivity results under visible irradiation indicate that the sample doped with NH₄Cl is the most selective photocatalyst. Therefore only the NH₄Cl-doped catalysts were tested under simulated solar light and near-UV radiation, so as to study the influence of the irradiation source.

Table 4 Reactivity results obtained under simulated solar irradiation

Catalysts	$Y^a/\text{mol}\%$		t^b/h		$X^c/\text{mol}\%$	$r_0^d/\text{mmol h m}^{-2}$
	10%	30%	10%	30%		
Degussa P25	21	18.5	0.25	0.8	87	0.00725
HP2	71	71	0.55	1.75	56	0.00084
N-HP0.1-NH ₄ Cl	90	76	1.0	2.5	41	0.00069
N-HP2-NH ₄ Cl	72	76	0.90	2.5	43	0.00095
N-HP5-NH ₄ Cl	75	71.5	0.45	1.5	71	0.00162
N-HP8-NH ₄ Cl	70	65	1.0	2.8	36	0.00083
N-HP2-NH ₄ Cl-400	25	24	1.1	2.9	25	0.00373
HPRT	64	64	0.7	2.5	39	0.00126

^a Selectivity for 10 and 30% MBA conversion. ^b Irradiation time for 10 and 30% MBA conversion. ^c MBA conversion after 3.5 h irradiation. ^d Initial oxidation rate of MBA.

Runs under simulated solar irradiation were carried out by using different catalysts prepared by varying the duration of the treatment at 100 °C. The reactivity results obtained with these samples are reported in Table 4; this table reports the selectivity to aldehyde for 10 and 30% MBA conversion and the irradiation time needed for 10 and 30% MBA conversion. The reaction rates under solar radiation are 2–3 times higher than that under visible radiation, as expected by considering that the light irradiance between 315 and 400 nm increases by about 4 times. The results of Table 4 indicate a detrimental effect on the selectivity at 30% conversion when the thermal treatment undergone by the photocatalyst lasted more than 2 h. The most active among the N-doped TiO₂ catalysts is N-HP5-NH₄Cl; this high reactivity could be due to the synergic effect of the presence of anatase and rutile phases.²⁸ This is probably due to the recombination rate decrease, caused by the interaction between the two different crystal phases (dimensions of anatase and rutile 4.5 and 10.2 nm, respectively). Even under simulated solar irradiation N-HP2-NH₄Cl showed a higher MBA disappearance rate with respect to the HP2 sample, thus confirming the positive role played by N-doping. Table 4 also shows that the most active catalyst is Degussa P25, but it is the least suitable one for the partial oxidation due to its lowest selectivity value, *ca.* 20%.

HPRT shows a similar photoactivity but a lesser selectivity with respect to the N-doped samples. The highest selectivity (90% at 10% conversion, see Table 4) was indeed reached by using the N-HP0.1-NH₄Cl sample. By considering the XRD patterns, HPRT is more crystalline than the doped catalysts although synthesised at room temperature. It should be considered that the HPRT preparation lasted for 6 days and this long time allowed a better crystallization with respect to other catalysts.

It is worth noting that both Tables 3 and 4 show that N-HP2-NH₄Cl activity and selectivity increased and decreased, respectively, when it underwent a thermal treatment at 400 °C and its crystallinity improved. This is indeed in agreement with previous literature.^{18–24}

The last series of experiments (Table 5) were performed under near-UV radiation. As the irradiance between 315 and 400 nm of this light source was 15–60 times higher than that of the other sources, the reactivities were the highest ones. The highest activity results were found with the N-HP2-NH₄Cl sample that is slightly less active than Degussa P25. Even if Degussa P25 and N-HP2-NH₄Cl catalysts show almost the

Table 5 Experimental results obtained under near-UV irradiation

Catalysts	$Y^a/\text{mol}\%$		t^b/h		$X^c/\text{mol}\%$	$r_0^d/\text{mmol h m}^{-2}$
	10%	30%	10%	30%		
Degussa P25	20	17	0.45	1.65	37	0.00618
HP2	73	72	0.20	0.5	68	0.00290
N-HP2-NH ₄ Cl	70	66	0.12	0.35	75	0.00585
HPRT	60	47	0.25	0.85	53	0.00353

^a Selectivity for 10 and 30% MBA conversion. ^b Irradiation time for 10 and 30% MBA conversion. ^c MBA conversion after 2 h irradiation. ^d Initial oxidation rate of MBA.

same reactivity, their selectivity values are quite different, the N-doped catalyst being four times more selective than P25 (66 *versus* 17%). These results clearly stress the point that an *a priori* correlation between reaction rate and selectivity cannot be made. The selectivity parameter depends on the catalysts surface distribution of mineralisation and partial oxidation sites.^{18,19}

Fig. 4–6 show representative runs of MBA oxidation with HP2, N-HP2-NH₄Cl and Degussa P25 catalysts under visible, simulated solar irradiation and near-UV light, respectively.

For the HP2 and N-HP2-NH₄Cl samples the reaction kinetics is of zero order under visible and solar radiation, while it is of first order under UV irradiation. The Degussa P25 sample instead showed first order kinetics under all three irradiation kinds. It must be stressed that the runs reported in these figures cannot be quantitatively compared among themselves as the irradiation conditions are different.

From all the photoreactivity results it may be concluded, as expected, that the increase of the UV radiation in the light source enhances overall reaction rate. The aldehyde production rate also obeys the same pattern. The results also show that the selectivity to aldehyde generally decreases by increasing the irradiation energy. This feature can be explained by considering that the mineralization reaction needs much more energy with respect to the partial oxidation one; as a consequence the more energetic UV irradiation should activate preferentially mineralization sites while visible radiation the partial oxidation ones.

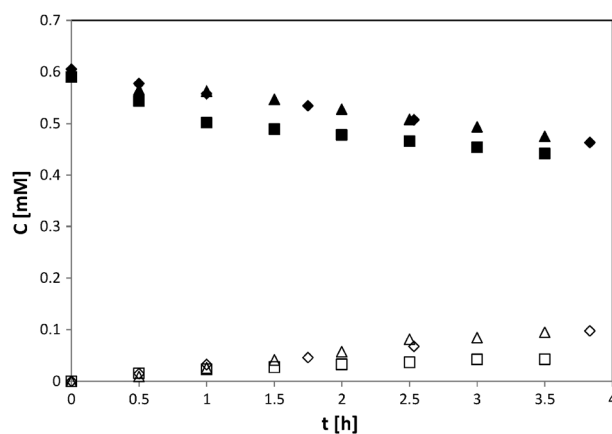


Fig. 4 Experimental results of representative runs of MBA oxidation with HP2 (◆,◇) N-HP2-NH₄Cl (▲,△) and Degussa P25 (■,□) catalysts under visible light. Symbols indicate the concentrations of MBA and PAA, respectively.

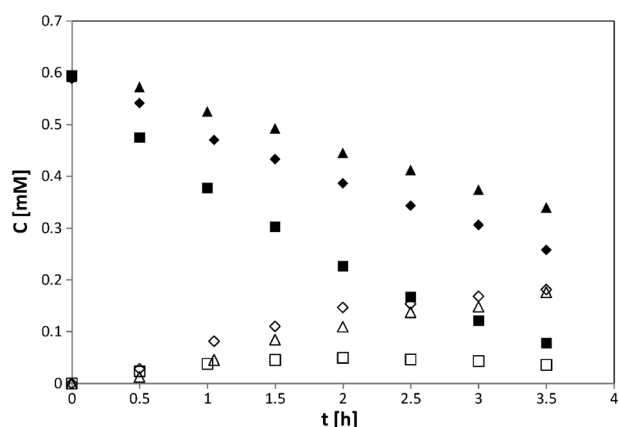


Fig. 5 Experimental results of representative runs of MBA oxidation with HP2 (◆,◇) N-HP2-NH₄Cl (▲,△) and Degussa P25 (■,□) catalysts under simulated solar irradiation. Symbols indicate the concentrations of MBA and PAA, respectively.

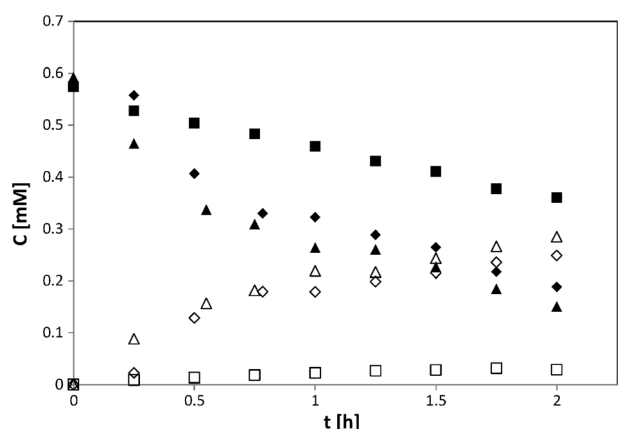


Fig. 6 Experimental results of representative runs of MBA oxidation with HP2 (◆,◇) N-HP2-NH₄Cl (▲,△) and Degussa P25 (■,□) catalysts under near-UV light. Symbols indicate the concentrations of MBA and PAA, respectively.

4 Conclusions

In this study the effect of N-doping of TiO₂ photocatalysts used to selectively convert MBA to PAA under different radiation sources and in pure water has been investigated. The results indicate that N-doping and exploitation of solar light, rather than UV-irradiation, are beneficial for enhancing the selectivity of partial oxidation of MBA to PAA. In particular poorly crystalline N-doped catalysts, prepared at low temperature by using NH₄Cl as nitrogen source, have been found to be the most selective samples, by reaching a 90% selectivity under simulated solar light. Thermal treatments yield an improvement in crystallinity and activity (in terms of initial disappearance rate) but, as the exploitation of UV light, are highly detrimental for selectivity. Finally doping with nitrogen together with calcination (see samples N-HP2-NH₄Cl-400 and N-HP2-Urea-400) does

not give rise to selective samples, due to a primary influence of particles sintering and higher crystallinity leading to high activity and low selectivity.

Notes and references

- 1 A. Fujishima, K. Hashimoto and T. Watanabe, *TiO₂ Photocatalysis, Fundamentals and Applications*, BKC Inc., Tokyo, 1999.
- 2 G. Palmisano, E. García López, G. Marci, V. Loddo, S. Yurdakal, V. Augugliaro and L. Palmisano, *Chem. Commun.*, 2010, **46**, 7074–7089.
- 3 L. Palmisano, V. Augugliaro, M. Bellardita, A. Di Paola, E. García López, V. Loddo, G. Marci, G. Palmisano and S. Yurdakal, *ChemSusChem*, 2011, **4**, 1431–1438.
- 4 *Heterogeneous photocatalysis*, ed. M. Schiavello, Wiley, New York, USA, 1995.
- 5 X. Qui and C. Burda, *Chem. Phys.*, 2007, **339**, 1–10.
- 6 M. Mrowetz, W. Balcerski, A. J. Colussi and M. R. Hoffmann, *J. Phys. Chem. B*, 2004, **108**, 17269–17273.
- 7 X. Chen, X. Wang, Y. Hou, J. Huang, L. Wu and X. Fu, *J. Catal.*, 2008, **255**, 59–67.
- 8 T. Olmez, *Fresenius Environ. Bull.*, 2008, **17**, 1789–1802.
- 9 M. Bellardita, M. Addamo, A. Di Paola, L. Palmisano and A. M. Venezia, *Phys. Chem. Chem. Phys.*, 2009, **11**, 4084–4093.
- 10 C. L. Bianchi, G. Cappelletti, S. Ardizzone, S. Gialanella, A. Naldoni, C. Oliva and C. Pirola, *Catal. Today*, 2009, **144**, 31–36.
- 11 Y. Yalcin, M. Kilic and Z. Cinar, *J. Adv. Oxid. Technol.*, 2010, **13**, 281–296.
- 12 O. S. Mohamed, A. E. M. Gaber and A. A. Abdel-Wahab, *J. Photochem. Photobiol., A*, 2002, **148**, 205–210.
- 13 S. Higashimoto, N. Kitao, N. Yohida, T. Sakura, M. Azuma, H. Ohue and Y. Sakata, *J. Catal.*, 2009, **266**, 279–285.
- 14 K. Sivarvanjani and C. Gopinath, *J. Mater. Chem.*, 2011, **21**, 2639–2647.
- 15 K. Yamaguchi and N. Mizuno, *Angew. Chem.*, 2002, **114**, 4720–4724 (*Angew. Chem., Int. Ed.*, 2002, **41**, 4538–4542).
- 16 G. J. ten Brink, I. W. C. E. Arends and R. A. Sheldon, *Science*, 2000, **287**, 1636–1639.
- 17 G. Palmisano, S. Yurdakal, V. Augugliaro, V. Loddo and L. Palmisano, *Adv. Synth. Catal.*, 2007, **349**, 964–970.
- 18 V. Augugliaro, H. Kisch, V. Loddo, M. J. López-Muñoz, C. Márquez-Álvarez, G. Palmisano, L. Palmisano, F. Parrino and S. Yurdakal, *Appl. Catal., A*, 2008, **349**, 182–188.
- 19 V. Augugliaro, H. Kisch, V. Loddo, M. J. López-Muñoz, C. Márquez-Álvarez, G. Palmisano, L. Palmisano, F. Parrino and S. Yurdakal, *Appl. Catal., A*, 2008, **349**, 189–197.
- 20 M. Addamo, V. Augugliaro, M. Bellardita, A. Di Paola, V. Loddo, G. Palmisano, L. Palmisano and S. Yurdakal, *Catal. Lett.*, 2008, **126**, 58–62.
- 21 V. Augugliaro, V. Loddo, M. J. López-Muñoz, C. Márquez-Álvarez, G. Palmisano, L. Palmisano and S. Yurdakal, *Photochem. Photobiol. Sci.*, 2009, **8**, 663–669.
- 22 S. Yurdakal, G. Palmisano, V. Loddo, V. Augugliaro and L. Palmisano, *J. Am. Chem. Soc.*, 2008, **130**, 1568–1569.
- 23 V. Augugliaro, T. Caronna, V. Loddo, G. Marci, G. Palmisano, L. Palmisano and S. Yurdakal, *Chem.–Eur. J.*, 2008, **14**, 4640–4646.
- 24 S. Yurdakal, G. Palmisano, V. Loddo, O. Alagöz, V. Augugliaro and L. Palmisano, *Green Chem.*, 2009, **11**, 510–516.
- 25 V. Loddo, S. Yurdakal, G. Palmisano, G. E. Imoberdorf, H. A. Irazoqui, O. M. Alfano, V. Augugliaro, H. Berber and L. Palmisano, *Int. J. Chem. React. Eng.*, 2007, **5**, A57.
- 26 S. Yurdakal, V. Loddo, G. Palmisano, V. Augugliaro, H. Berber and L. Palmisano, *Ind. Eng. Chem. Res.*, 2010, **49**, 6699–6708.
- 27 D. Mardare, D. Luca, C.-M. Teodorescu and D. Macovei, *Surf. Sci.*, 2007, **601**, 4515–4520.
- 28 T. Ohno, K. Sarukawa, K. Tokieda and M. Matsumura, *J. Catal.*, 2001, **203**, 82–86.